NONLINEAR DEFORMATION AND STABILITY OF OVAL CYLINDRICAL SHELLS UNDER PURE BENDING AND INTERNAL PRESSURE

L. P. Zheleznov, V. V. Kabanov, and D. V. Boiko

UDC 629.7.023:539.4.384.4

The stability problem of a cylindrical shell of oval cross section loaded by a bending moment and internal pressure is studied. The variational displacement finite-element method is used. For the prebuckling stress–strain state, the bending and nonlinearity are taken into account. The effects of the nonlinear nature of the deformation and the cross-sectional ovality of the shells on the critical loads and buckling modes are determined.

Key words: oval cylindrical shell, bending moment, internal pressure, nonlinear deformation, stability, finite-element method.

Introduction. Noncircular cylindrical shells are much more economical than circular shells. The use of these shells in the structures of modern passenger airplanes makes it possible to use the space of the air-tight cabin more effectively, improve comfort, increase the seating capacity, and reduce the mass of the plane. An example is the 500 seat A-380 airbus with a double-deck air-tight cabin of oval cross section. However, no reliable methods for the stability analysis of these air-tight cabins have not been developed since, unlike for circular cylindrical shells, the buckling behavior of noncircular shells is not well understood. The reason is that the problems are difficult to solve because the variable curvature radius of noncircular shells leads to variable coefficients in the buckling equations. The well-known solutions of shell buckling problems were obtained by analytical methods and, as a rule, in a linear approximation ignoring the prebuckling bending and nonlinearity, i.e., in the classical formulation. The loading of oval cylindrical shells considered in the present paper has not been studied even in the classical formulation.

Nonlinear Deformation and Stability of Unstiffened Shell. We consider the nonlinear deformation and stability of a cantilevered ($u = v = w = w_x = 0$) cylindrical shell of oval cross section subjected to internal pressure q and end bending moment M. The loaded end of the shell is reinforced by a ring stiffener which is rigid in its plane. The bending moment is represented by the axial load $T = M z_1 / J$ distributed nonuniformly along the shell director (z_1 is the distance from the cross-sectional contour to the horizontal axis AA and J is the moment of inertia of the cross-sectional area about the axis AA). The shell has a length $L = 2800$ mm, a thickness $h = 3.3$ mm, an elastic modulus of the material $E = 7 \cdot 10^4$ MPa, and Poisson's ratio $\nu = 0.3$.

We consider an oval with semiaxes a and b (Fig. 1) composed of two pairs of circumferences in the following manner. A circumference of radius a with center O is drawn to intersect the semiaxis b. A circumference of radius $a - b$ is then drawn to intersect the line AB. The section AC is divided into halves and a perpendicular to it is erected. Circular arcs of small radius r and large radius R centered at O_r and O_R, respectively, are drawn. The point at which the circular arcs are conjugated is defined by an angle α. The thus constructed oval has the geometrical characteristics

$$r = a\,\frac{1 + k^2 - \sqrt{1 + k^2}}{1 + k - \sqrt{1 + k^2}}, \qquad R = a\,\frac{1 - k(\sqrt{1 + k^2} - k)}{1 + k - \sqrt{1 + k^2}}, \qquad k = \tan\alpha = \frac{b}{a}.$$
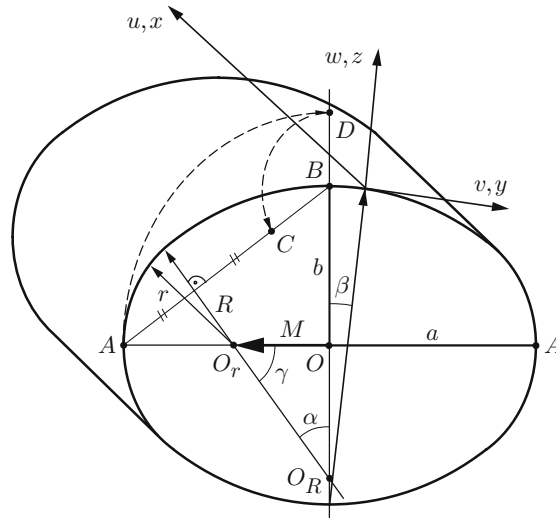
Fig. 1. Geometry of the oval.

The perimeter of the oval is $P = 4(R\alpha + r\gamma)$, where $\gamma = \pi/2 - \alpha$. The radius of a circle of the same perimeter (equiperimetric radius) is $R_0 = P/(2\pi) = 1000$ mm.

To solve the problem numerically, we employ the modified variational displacement finite-element method proposed in [1, 2]. This method uses an effective quadrilateral shell finite element of natural curvature, for which rigid-body displacements are written explicitly in approximating the displacement field. The principal-curvature lines divide the shell into m parts along the generatrix and n parts along the director. The shell is thus represented by a set of $m \times n$ finite elements. The deformation displacements of the finite element are approximated by polynomials. The problem reduces to a system of nonlinear algebraic equations for the nodal unknowns of the elements. This system is solved by a step-by-step method by varying the load and involving linearization of the system at each step according to the Newton–Kantorovich method. The linear system is solved by the Kraut method using decomposition of the Hesse matrix (the matrix of the second derivatives of the potential strain energy of the shell) $H = LDL^{\mathrm{t}}$ into diagonal and two triangular matrices. The stability of the shell is checked by investigating the positive definiteness of the Hesse matrix according to the Sylvester criterion, which reduces to checking the positive definiteness of the elements of the diagonal matrix D. The occurrence of negative elements indicates instability of the shell. Once the load for which the equilibrium state becomes unstable is found, the buckling mode of the shell is determined by solving the system $H\boldsymbol{\delta} = 0$, where $\boldsymbol{\delta}$ is the bifurcational nodal displacement vector. To this end, a linear-dependent (degenerate) row of the matrix H that corresponds to the first negative element of the matrix D is determined. The elements of this row and the corresponding column of the matrix H are set equal to zero. The diagonal coefficient is replaced by unity, and the corresponding column multiplied by the prebuckling displacement corresponding to the degenerate row is taken as the right side of the system. Solution of the resulting system yields the buckling mode of the shell. In the limit-point case, the failure mode is found from the basic nonlinear stress–strain state for a load close to the limit load.

Convergence of the solution with respect to the number of finite elements is given by

$m \times n =$	5×120	10×120	20×120	30×120
Δ, % $=$	30	5	1	0.5

(Δ is the error). Because of the symmetry of the loading, a quarter of the shell was considered with the imposition of symmetry conditions along the edges.

Figure 2 shows the parameters $k_m = M_0^*/M_0$ and $k_q = q/q_e$ versus the parameter $\bar{a} = a/b$ for separate action of the loads [q and M_0^* are the critical internal pressure and bending moment, respectively, $q_e = \bar{q}E\gamma^2$, $\bar{q} = (24.1k + 130.2k^3 + 276.3k^5)\lambda^{-2}\gamma^{0.6}$, $\lambda = L/R_0$, $\gamma = h/R_0$, $k = b/a \leqslant 1$, and $M_0 = \pi ER_0h^2/\sqrt{3(1 - \nu^2)}$ is the critical bending moment for a circular cylindrical shell of radius R_0]. One can see that for the action of internal pressure, the effect of the nonlinear initial stress–strain state of elliptic shells is pronounced in the ranges
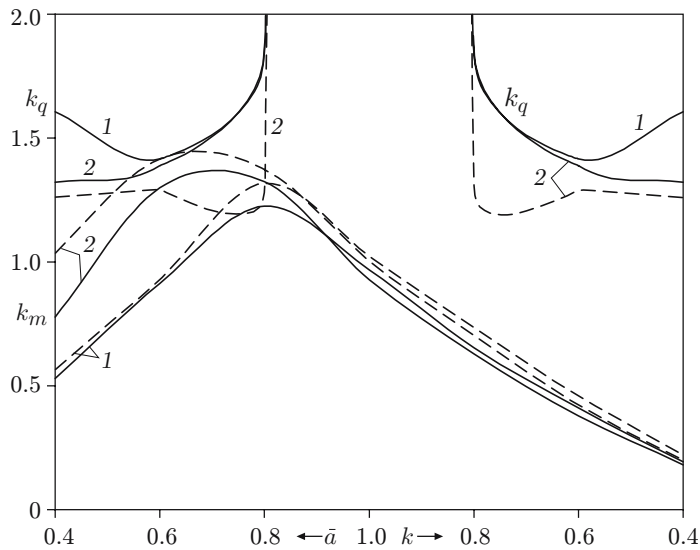
Fig. 2. Parameters k_m and k_q versus the parameter $\bar{a}$ for separate action of the loads: curves 1 refer to equiperimetric oval shells and curves 2 refer to elliptic shells; the dashed and solid curves refer to the linear and nonlinear initial stress–strain states, respectively.
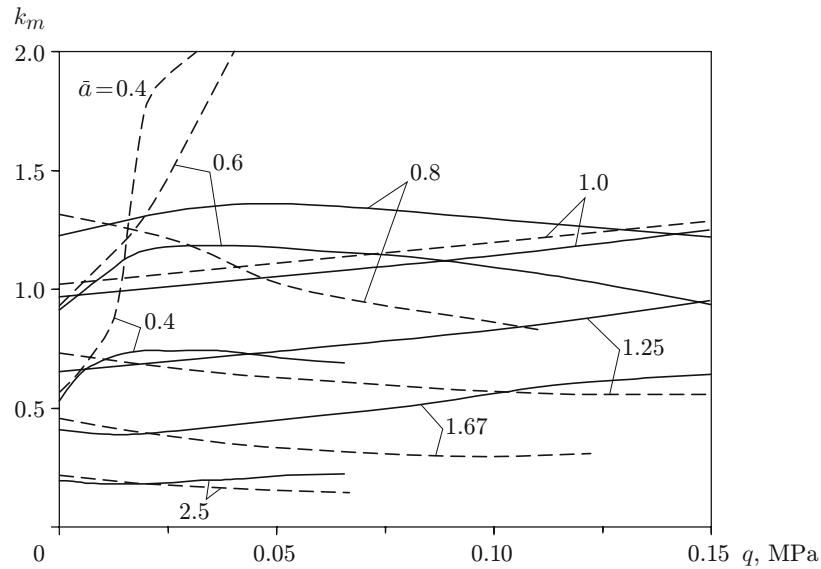

Fig. 3. Parameter k_m versus the internal pressure q for oval shells.

$0.6 < \bar{a} < 0.8$ and $1.675 > \bar{a} > 1.25$. For oval shells, the critical values of the internal-pressure parameter k_q exist only for the nonlinear initial stress–strain state. The critical values of k_q for oval shells are higher than those for equiperimetric elliptic shells. In the range $0.8 < \bar{a} < 1.25$, no buckling occurs for both elliptic and oval shells under the action of internal pressure.

For the action of the bending moment, the effect of nonlinearity is pronounced for elliptic shells with $\bar{a} < 0.8$ and oval shells with $0.9 > \bar{a} > 0.7$. In the range $\bar{a} < 0.8$, the critical values of k_m for oval shells are much lower than those for elliptic shells. Due to the nonlinear effects, the critical internal pressure increases and the critical bending moment decreases.

Figure 3 shows the parameter $k_m = M_0^*/M_0$ versus the internal pressure q for oval shells for various values of the parameter $\bar{a}$ (the dashed and solid curves refer to the linear and nonlinear prebuckling stress–strain states, respectively). One can see that for oval shells, the effect of the nonlinear stress–strain state is of a complex nature.
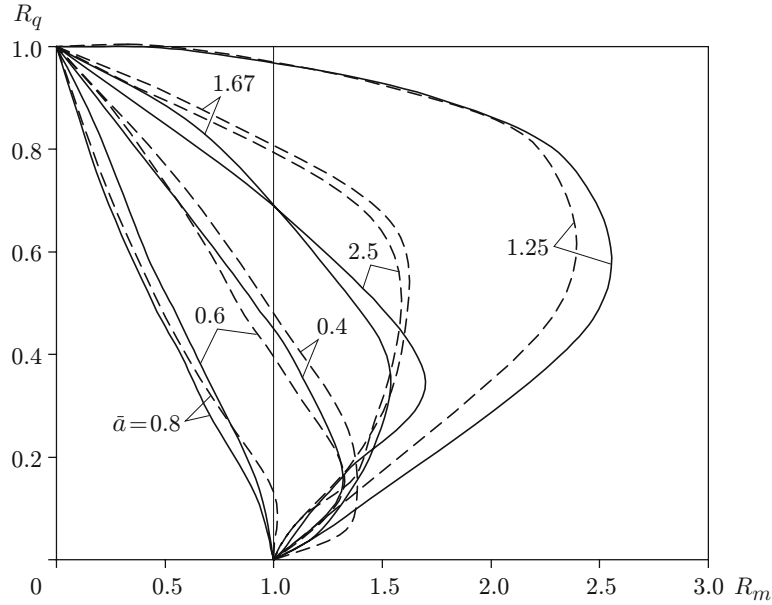
408

Fig. 4. Curves of $R_q(R_m)$ for oval shells (solid curves) and elliptic shells (dashed curves).

In most cases, the curves based on the linear solution are higher than those based on the nonlinear solution. For high values of the internal pressure ($q > 0.05$), oval shells with $\bar{a} = 0.4$ and 0.6 do not buckle for the linear stress–strain state. Moreover, one can see from Fig. 3 that for $\bar{a} > 1$, the critical values of the parameter k_m increase with increasing q. In this case, the internal pressure has a supporting effect on the shell. For $\bar{a} < 1$, a high internal pressure decreases the critical moment. This pattern of the curves is also typical of elliptic shells.

Figure 4 shows curves of $R_q(R_m)$ for oval and elliptic shells (solid and dashed curves, respectively) obtained with allowance for the nonlinear stress–strain state for various values of the shell parameter $\bar{a}$ ($R_q = k_q/k_{q0} = q/q_0$, $R_m = k_m/k_{m0} = M^*/M_0^*$, $k_q = q/q_e$, $k_m = M_0^*/M_0$, k_{q0} and k_{m0} are the critical values of the parameters k_q and k_m, respectively, and q_0 and M_0^* are the critical values of q and M for separate loading). The points of these curves correspond to the critical values of the parameters of internal pressure and bending moment. Most of the curves have two characteristic segments, each which describe different effects of internal pressure on the stability of the shells. This segments are separated by the vertical line $R_m = 1$, on which the pressure has no effect. For $R_m > 1$, the pressure increases the buckling strength of the shells by exerting a supporting effect, and for $R_m < 1$, it decreases the critical moment.

From Fig. 4, one can also see that the internal pressure load decreases the critical bending moment for $\bar{a} < 1$ (vertically elongated shells) and increases it for $\bar{a} > 1$ (flattened shells). This can be explained by the location of the critical zones (instability zones) for the internal pressure and bending moment. For the internal pressure load, these zones are closer to the zones of large-curvature shells, and for the bending moment, they are in the compression regions in the upper part of the shell. For elongated shells, the critical zones corresponding to the pressure and bending are more overlapped than those for flattened shells. In addition, for flattened shells, the tensile zones due to the internal pressure are overlapped by the compression zones due to bending, thus increasing the buckling strength of the shell.

The fact that the internal pressure has an ambiguous effect on the segments of the curves $R_q(R_m)$ for $R_m > 1$ is of interest. The curves of $R_q(R_m)$ are the boundaries between the stability and instability regions of the shells. A shell stable for a given value of $R_m > 1$ can buckle under both decreasing and increasing internal pressure.

Figure 5 shows the buckling modes of shells for $q = 0.06$ MPa and $\bar{a} = 0.8$ (a) and 1.25 (b). The buckling mode depends strongly on the ratio k_q/k_m. Shells elongated in the vertical direction buckle in the compression zone with the formation of several inclined wrinkles expending over the entire length of the shell, and flattened shells buckle in the zone of maximum compressive longitudinal stresses, as in the case of pure bending. (The results were obtained for an $m \times n = 30 \times 60$ finite-element mesh, which ensures convergence of the solution.)
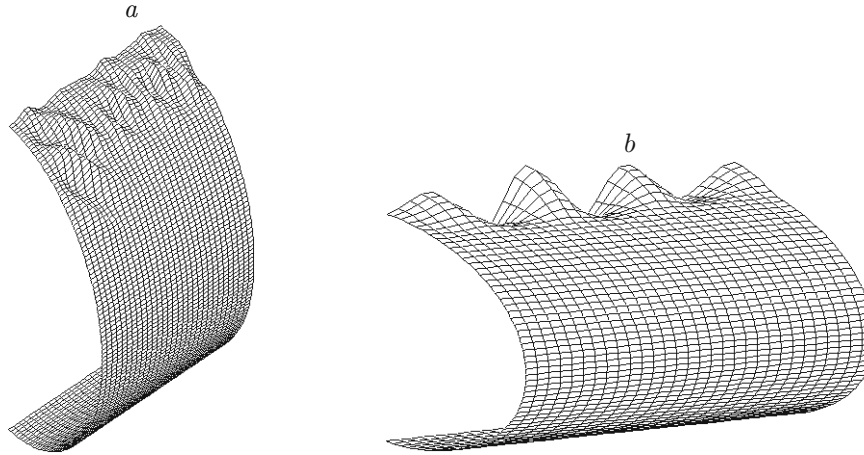
Fig. 5. Buckling modes of shells elongated (a) and flattened (b) in the vertical direction.
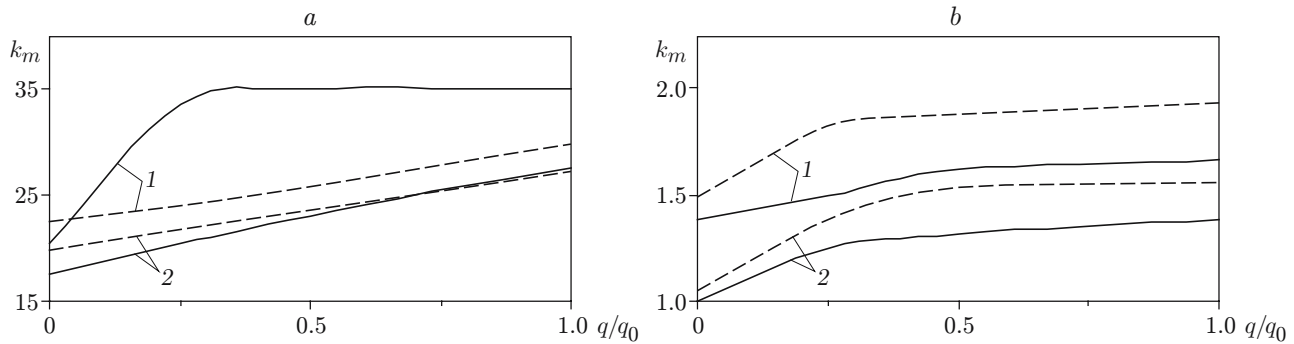

Fig. 6. Parameter k_m versus the parameter q/q_0 for $F_s > 0$ (a) and $F_s = 0$ (b).

Strength and Buckling Analysis of a Fuselage Section of a Passenger Airplane. As an example, we consider a stringer-stiffened oval fuselage section of a passenger airplane. The section is a shell composed of three pairs of circumferences of radii equal to 1810, 1900, and 2700 mm. The oval contour is close to an elliptic contour with semiaxes $a = 1900$ mm and $b = 2050$ mm. The section (below referred to as the shell) has a length $L = 500$ mm (ring stiffener spacing) and a thickness $h = 3.2$ mm and is made of a material with an elastic modulus $E = 0.7 \cdot 10^4$ MPa and Poisson's ratio $\nu = 0.3$. The cross-sectional area of the stringers is $F_s = 306$ mm^2, the moment of inertia $J_s = 41,000$ mm^4, the stringer spacing $d_s = 150$ mm, and the eccentricity (the distance between the centroid of the stringer cross section to the mid-surface of the shell) is $e_s = 10$ mm. The shell is loaded by internal pressure q and bending moment M acting in the vertical or horizontal plane and is treated as a structurally anisotropic shell [3].

Figure 6 shows the parameter $k_m = M^*/M_0$ versus the parameter q/q_0 (M^* is the critical bending moment, $M_0 = 2 \cdot 10^9$ N·cm, and $q_0 = 0.2$ MPa) for stiffened shell ($F_s > 0$) and unstiffened shell ($F_s = 0$) for the linear and nonlinear prebuckling states (dashed and solid curves, respectively). Curves 1 refer to the bending moment applied in the vertical plane and curves 2 refer to that in the horizontal plane. One can see that the critical moment in the vertical plane of the stiffened shell is higher than that in the horizontal plane. For small values of the parameter q/q_0, the effect of nonlinearity is greater for the stiffened shell than for the unstiffened shell. In the case of the bending moment acting in the vertical plane, the prebuckling nonlinearity increases the critical load for the stiffened shell and decreases it for the unstiffened shell. For the bending moment acting in the horizontal plane, the effect of nonlinearity is greater for unstiffened shell.
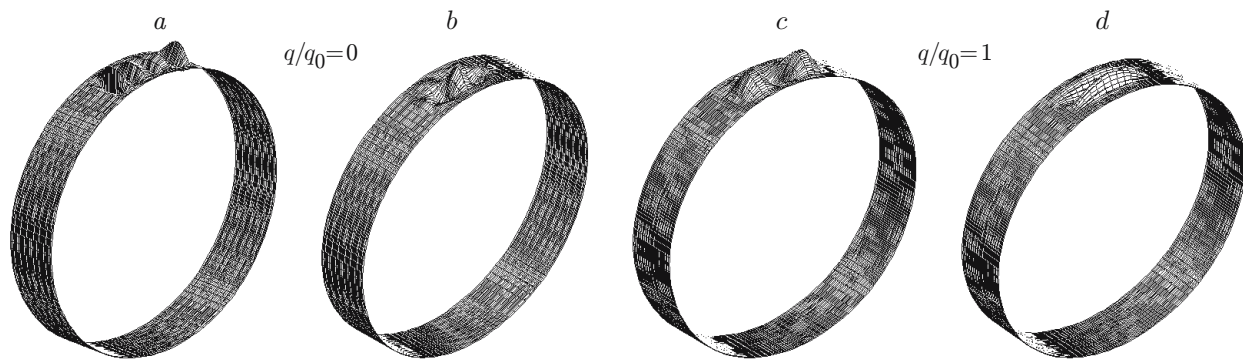
Fig. 7. Buckling modes of stiffened (a and c) and unstiffened (b and d) shells subjected to the bending moment in the vertical plane.

Figure 7 shows the buckling modes of unstiffened and stiffened shells subjected to bending in the vertical plane for $q/q_0 = 0$ (a and b) and 1 (c and d). One can see that buckling occurs in the upper part of the shell, where the maximum compressive normal stresses are reached. Moreover, the buckling mode is affected qualitatively by the stiffeners and internal pressure. For example, stiffened shells buckle with the formation of two waves along the arc (Fig. 7a) in the absence of internal pressure and with the formation of one wave in the presence of internal pressure (Fig. 7c). Unstiffened shells buckle with the formation of a half-wave in the upper part (Fig. 7b) in the absence of internal pressure and with the formation of two half-waves (Fig. 7d) in the presence of internal pressure.

REFERENCES

1. L. P. Zheleznov and V. V. Kabanov, "Finite element and algorithm for studying the nonlinear deformation and stability of noncircular cylindrical shells," in: *Applied Problems of Mechanics of Thin-Walled Structures* [in Russian], Izd. Mosk. Univ., Moscow (2000), pp. 120–127.
2. L. P. Zheleznov and V. V. Kabanov, "Nonlinear deformation and stability of noncircular cylindrical shells under internal pressure and axial compression," *J. Appl. Mech. Tech. Phys.*, **43**, No. 4, 617–621 (2002).
3. V. V. Kabanov, *Stability of Heterogeneous Cylindrical Shells* [in Russian], Mashinostroenie, Moscow (1982).